Available online at www.sciencedirect.com
ScienceDirect
Ceramics International 36 (2010) 1383–1388
CERAMICS INTERNATIONAL
www.elsevier.com/locate/ceramint

Mechanism of seeded infiltration growth process analysed by magnetic susceptibility measurements and in situ observation

Haitao Cao [a,b,*], X. Chaud [c], J.G. Noudem [b], Cuiping Zhang [a], Rui Hu [a], Jinshan Li [a], Lian Zhou [a]

[a] The State Key Laboratory of Solidification Processing, Northwestern Polytechnical University, Shaanxi, Xi'an 710072, PR China
[b] Laboratory of Crystallography and Material Sciences-CRISMAT-CNRS UMR 6508 6, Boulevard du Maréchal Juin, 14050 CAEN Cedex, France
[c] CRETA/CNRS, 25 Av des Martyrs, 38042 Grenoble Cedex 09, France

Received 14 September 2009; received in revised form 25 November 2009; accepted 24 January 2010
Available online 3 March 2010

Abstract

Using the magnetic susceptibility measurements (MSM) at high temperature and in situ video observation, the mechanism of seeded infiltration growth (SIG) process was investigated. This process offers the opportunity to verify the main phase transition by measuring the magnetic force acting on the sample. The heat treatment process which adjusted from MSM and video observation, allows to obtain the single domain YBCO superconductor.

Keywords: SIG mechanism; Magnetic susceptibility; Video observation; Superconductor; YBCO

1. Introduction

It is well known that the microstructure of plain bulk superconductors should be free of defects, such as cracks, pores and voids, in order that the sample can trap high magnetic field or carry high current densities. For studying and minimize the above defects, the combination of standard superconducting ceramic process and a seeded infiltration growth (SIG) technique, to prepare $YBa_2Cu_3O_{7-x}$ (Y123) bulk superconductors has been reported [1–5]. This process involves negligible shrinkage and a uniform distribution of Y_2BaCuO_5 (Y211) inclusions.

Melt-textured YBCO bulk superconductor fields are highly attractive for practical application due to high critical current density J_c and high trapped magnetic field. The preparation of single domain YBCO using conventional melt processing and high trapped magnetic field has been reported [6–9]. The main characteristic of the conventional processing is to peritectically decompose the material above the melting temperature of Y123 and grow the single domain by using the low cooling rate. SIG process was introduced by Chen [4], and its remarkable advantage is that with SIG process, the macro-defects, voids in the sample can be reduced significantly and the shrinkage can be neglected. The SIG process can also produces effective pinning centers in the microstructure of YBCO bulk superconductors, and leading directly to high J_c values at 77 K [1–5].

But the mechanisms of nucleation and growth of SIG process are not clear. There are still many problems in growing large samples because parameters change from one composition to another and an accurate determination of the solidification range is necessary. The accurate determination of the phase transitions of MTG YBCO bulk in situ video observation for real processing conditions enabled the growth of large single domain YBCO bulk sample up to 93 mm [10]. MSM can be used to know clearly the phase transition at the real time during the SIG process and understand better the growth mechanisms. Then combining the in situ observation, we can optimize the heat treatment for a given composition and precursor [11].

In this paper, MSM was used to monitor the phase transition and then according to the results of the MSM curve, the mechanisms of the SIG process were investigated by (i) magnetic susceptibility measurements at high temperature and (ii) in situ video recorded during process. The heat treatment process was adjusted and allows to obtain the single domain YBCO superconductor.

* Corresponding author at: Laboratory of Crystallography and Material Sciences-CRISMAT-CNRS UMR 6508 6, Boulevard du Maréchal Juin, 14050 CAEN Cedex, France. Tel.: +33 231 45 13 66; fax: +33 231 95 16 00.
E-mail addresses: haitao.cao@ensicaen.fr, caohaitaoapple@hotmail.com (H. Cao).

0272-8842/$36.00.
doi:10.1016/j.ceramint.2010.02.009

2. Experimental procedure

The samples for infiltration process have been prepared using commercial powders Y123 (SR 30, Solvay, purity 99.9%), Y211 (Nexans, purity 99.9%). The weights of Y123 and Y211 powders are15 g and 12.5 g, respectively. The powder was then pressed uniaxially into pellets of 16 mm in diameter. In order to isolate the sample from the Al_2O_3 substrate and prevent the parasitic nucleation, the buffer layer of approximate thickness 2 mm were prepared from a mixture of Y_2O_3 and Yb_2O_3 with a nominal composition of Y_2O_3:Yb_2O_3 = 1:1.

The MSM is performed in specially designed furnace combining high temperatures and the high magnetic field (maximum 8 T) given by a superconducting Oxford coil (Fig. 1).

The magnetic susceptibility is derived by measuring the force which a strong magnetic field gradient exerts on it. The force acting on the sample is given by $F = \chi B\, dB/dz$, where the $B\, dB/dz$ is a constant (263.618 T^2/m) [12] depending on the coil. The magnetic force is measured by an electronic balance with a 1200 g capacity and a 1 mg resolution. We assume that magnetic behavior of the sample is due to a change of the copper valency from non-magnetic Cu^+ ions to paramagnetic Cu^{2+} as the oxygen content in the liquid evolves [13].

The SIG-YBCO sample is put on a substrate with a mixture of Y_2O_3 and Yb_2O_3 powder layer. The total signal (S) measured from the balance is as follows:

$$S_{\text{signal}} = W(\text{sample weight}) + F(\text{sample magnetic force}) + [W'(\text{substrate and crucible weight}) + F'(\text{substrate and crucible magnetic force})].$$

The signal of substrate and crucible is less than 6% of the total signal, consequently, S_{signal} can be used for studying the susceptibility transition of YBCO sample. In this paper, we used S_{signal} as Y-axis and normalized the Y-scale with the sample mass; the unit of Y-scale is g/g which represents the weight and force signal per gram referred as "S_{signal}(g/g)". The Y-scale of thermogravimetry is also normalized by mass; the unit is as g/g.

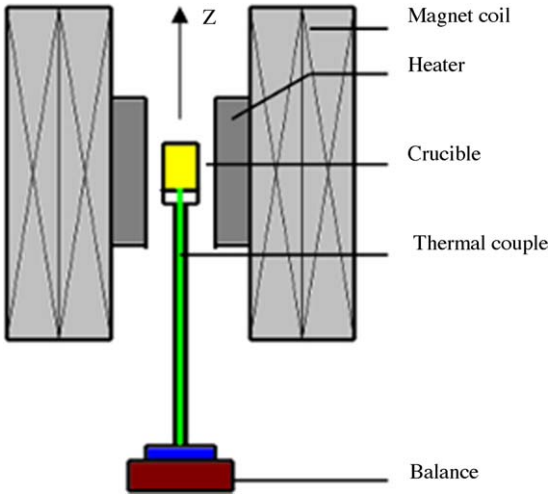

Fig. 1. Sketch of equipment of MSM. Faraday balance in CRETA; maximum magnetic field: 8 T; maximum temperature: 1200 °C

3. Results and discussion

3.1. Magnetic susceptibility measurements

The high temperature susceptibility has been performed using the conventional SIG configuration. In this experiment, the cooling rate was fixed at 2 °C/h with respect to 0.5 °C/h commonly used [1]. First, two magnetic susceptibility curves of bulk samples with seed and without seed are measured. The idea here is to investigate the nucleation temperature with or without seeding the sample. As shown in the Fig. 2(a), at point A (T = 1000 °C), Y123 phase begins to be decomposed into Y211 and liquid phase (L = $Ba_3Cu_5O_x$) until the point B (T = 1050 °C). The reaction is:

$$\text{Y123} \rightarrow \text{Y211} + \text{L}$$

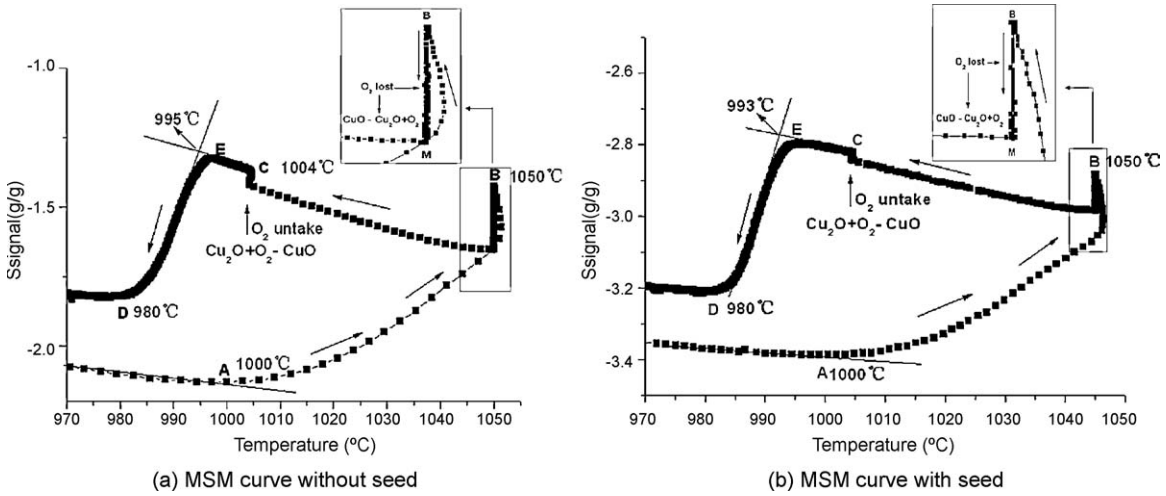

Fig. 2. MSM curves of the bulk samples during the SIG process. (a) MSM curve without seed; (b) MSM curve with seed.

So the melting region is from A point to B point. As we all know, Y123 crystal contains Cu^{3+} and Cu^{2+} ions. So the increase of susceptibility can just explained by the contribution of the Cu^{2+} ion susceptibility based on the change of Cu^{3+} to Cu^{2+} during this melting period. When there is overheating in the sample after melting, the magnetic susceptibility (the curve part above the melting point B) does not abide by a Curie–Weiss law. The reason is the oxygen flowing out of the sample according to the reaction:

$$CuO \rightarrow Cu_2O + O_2$$

It is because non-magnetic Cu^{+} ions change to paramagnetic Cu^{2+}. Until the point C (1004 °C), because of the oxygen uptake ($Cu_2O + O_2 \rightarrow CuO$), the susceptibility curve has a notable change. At point C, the Y123 crystal begins nucleating, and the small tiny crystals can be seen at the sample top surface monitored by the in situ observation method at point C. But, only if the growth of Y123 crystal reaches certain proportion of the total bulk volume (around 2%), the susceptibility can exhibit the obvious change. That is why there is an obvious change from point E to point D (solidification range). The susceptibility changes quickly as the solidification process is triggered at point E. After compared with the results of the MSM curve with seed (Fig. 2(b)), the difference cannot be seen from these two curves.

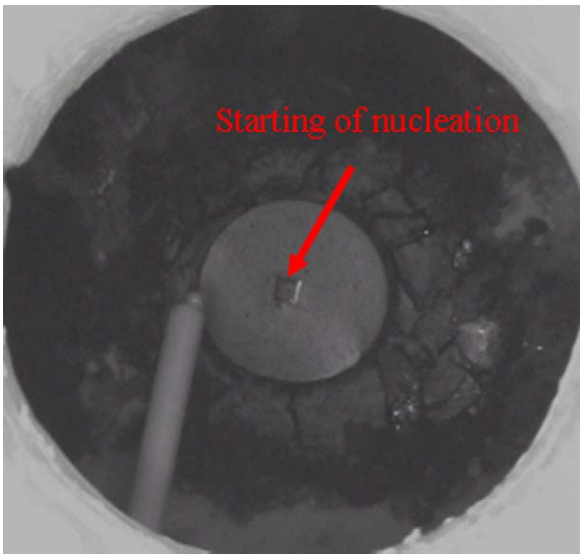

Fig. 3. Picture of the starting of nucleation.

During the course of cooling, you can see a little difference at the nucleation temperature from the top surface of the sample. In the case of sample without seed, the crystal can nucleate anywhere inside the sample, but for the sample with seed, the crystal nucleates where was the seed (in the case of

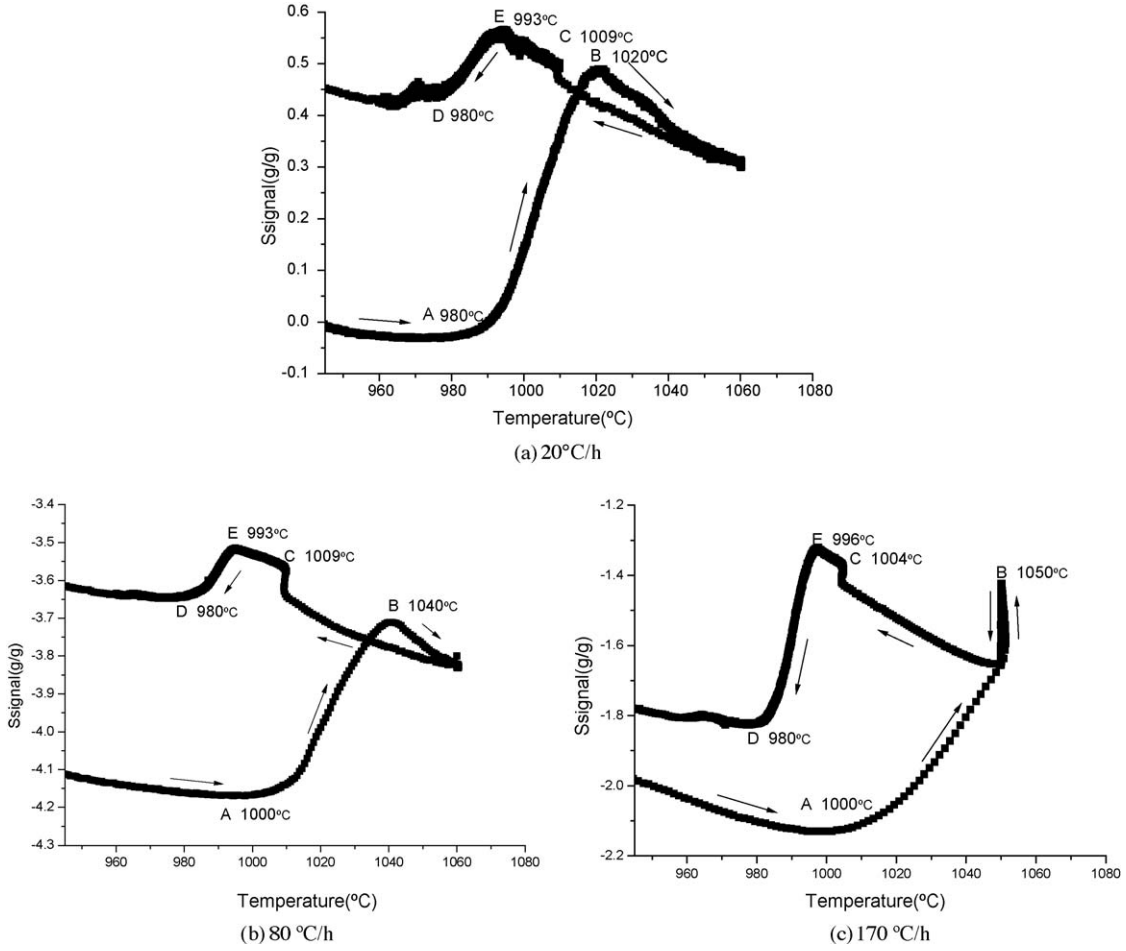

Fig. 4. Susceptibility curves of SIG (without seed) with different heating rate of 20 °C/h, 80 °C/h, and 170 °C/h.

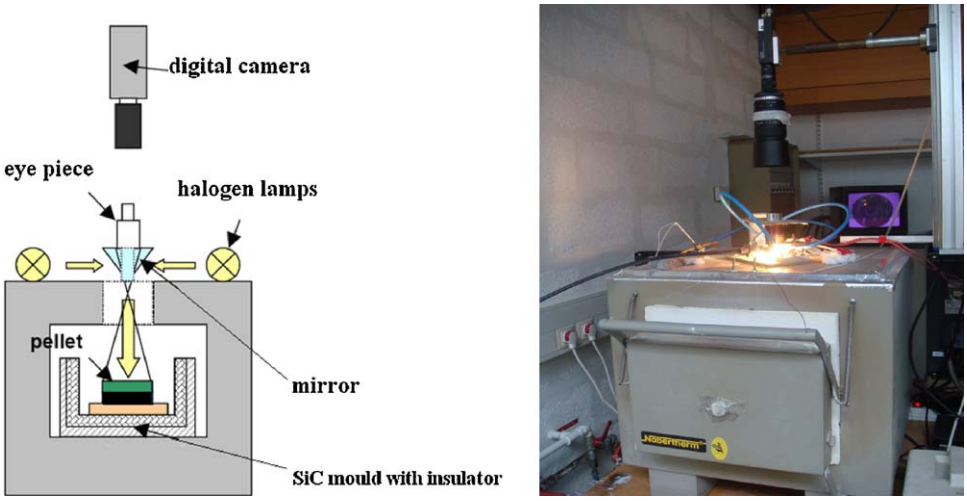

Fig. 5. Sketch and equipment of in situ observation.

Fig. 3), then after nucleation, the crystal will grow along the ab plane and c axis and at the same time, the heterogeneous nucleation and growth can be suppressed. The effect of the seed can increase the nucleation temperature (above the 1004 °C). But it cannot be displayed in the MSM curves.

Different heating rates (20 °C/h, 80 °C/h, 170 °C/h) from 945 °C to 1100 °C were investigated (as shown in the Fig. 4). From the results, it can be seen clearly, at the lower heating rate, the melting region (from A to B point) and the initial nucleation point could be changed. For the rate of 170 °C/h used as conventional SIG heat treatment, the melting region is from 1000 °C to 1050 °C (A to B), and the solidification region is from1004 °C to 980 °C (C to D). But for the rate of 20 °C/h and 80 °C/h, the melting region is from 980 °C to 1020 °C and from 1000 °C to 1040 °C, respectively. The solidification region is the same, from 1009 °C to 980 °C.

For the lower heating rate, the sample has enough time to respond to the change of temperature and to finish the whole melting course of sample. But for the higher heating rate, the sample has no enough time to react, just only a part of bulk sample melt. So when the sample has enough liquid phases, it is easier for the reaction between the liquid source and the seed, and to nucleate earlier under the place of seed. This is the reason why the initial transition point in the magnetic susceptibility curve increased.

3.2. *In situ video observations*

We used the equipment of Fig. 5 to prepare the sample. The whole infiltration process was monitored at high temperature using camera fixed on the top of furnace (Fig. 5(b)). By combining the MSM analysis and the furnace used for video observation, the heat treatment was adjusted at 996 °C and kept at this temperature until the end (by observation) of the crystal growth. After this stage, the furnace was cool down as usual.

In the other hand, the samples were quenched at different stages during the SIG process (Fig. 6). For the first experiment, the sample was ramped to 1050 °C at a rate of 200 °C/h and held for 0.5 h (Fig. 6(a)), during this stage the source compact incongruently melts and the barium cuprate liquid infiltrates the porous Y-211 pre-form and the reaction with Y211 started. Fig. 6(b) shows the sample quenched after holding 1 h at 1050 °C, the liquid phase fully infiltrated into the Y211 according to the chemical reaction L + Y211 → Y123. One can observe on the microstructure some regions are rich in liquid phase compare to some area where the Y123 is completely formed. The third sample quenched at 1000 °C during solidification clearly shows that all the Y211 and liquid phase have been converted into Y123.

In addition, the sample quenched at the dwelling time (996 °C) is presented at the Fig. 7a. From the picture, the clear

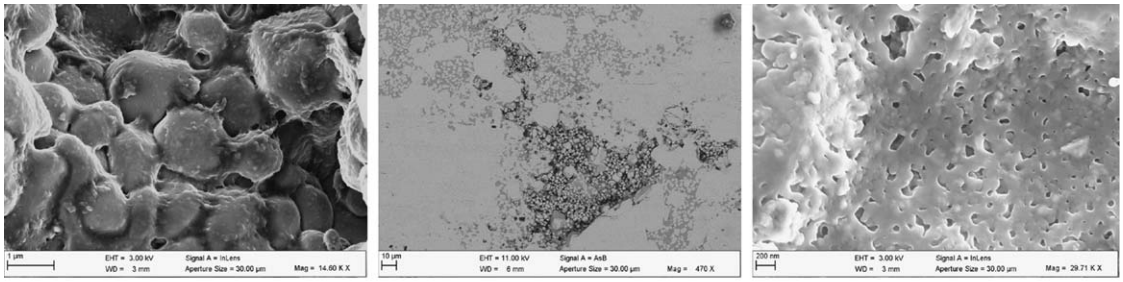

(a) holding 0.5h at 1050°C (b) holding 1h at 1050°C (c) at 1000°C

Fig. 6. Microstructure of the sample quenched at different stages during the SIG process. (a) Holding 0.5 h at 1050 °C; (b) holding 1 h at 1050 °C; (c) at 1000 °C.

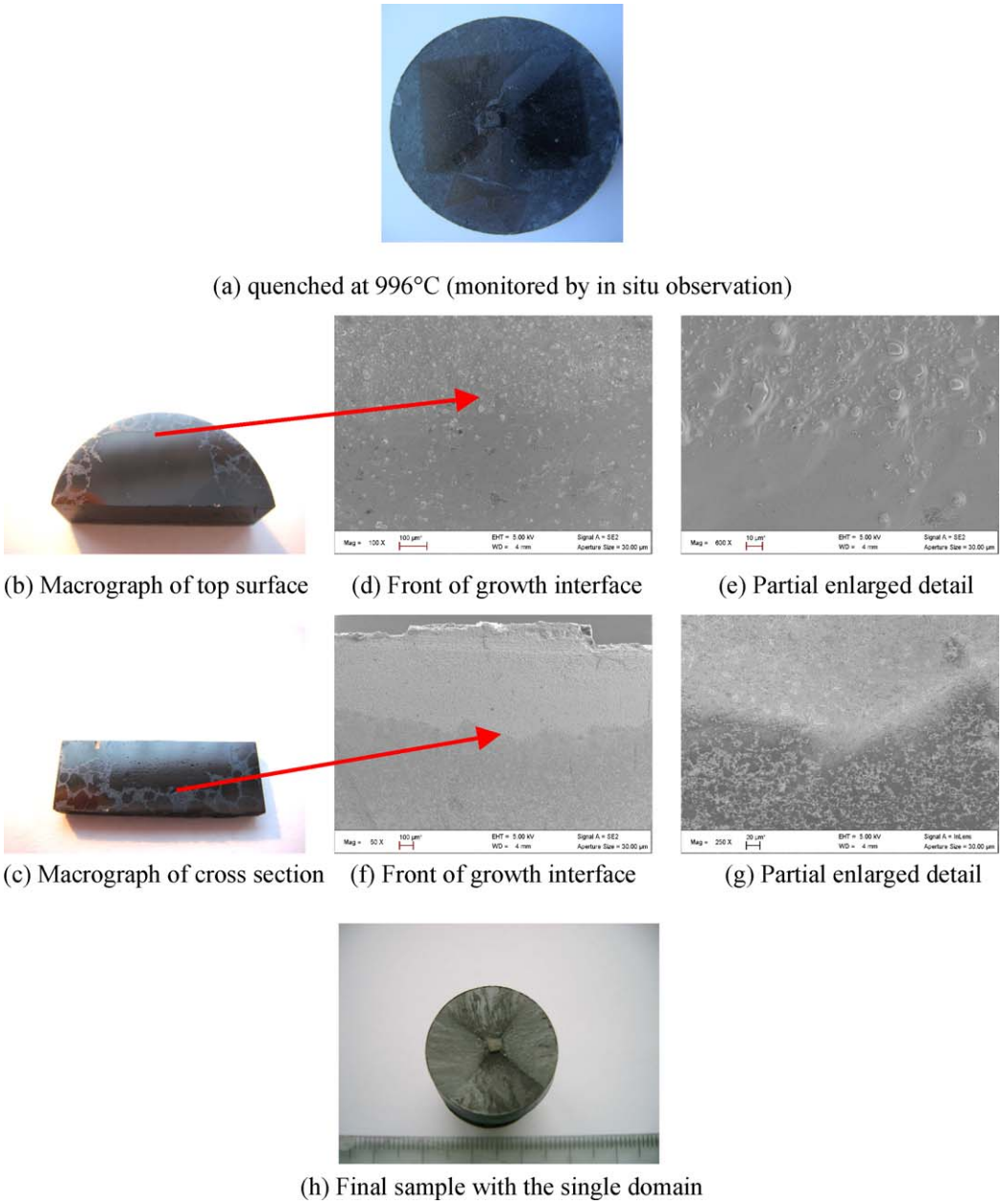

Fig. 7. Macrograph and microstructure of the sample quenched at 996 °C and the sample with single domain (monitored by in situ observation): (a) quenched at 996 °C (monitored by in situ observation); (b) macrograph of top surface; (c) macrograph of cross-section; (d) front of the growth interface of top surface; (e) partial enlarged detail of top surface; (f) front of the growth interface of cross-section; (g) partial enlarged detail of cross-section; (h) final sample with the single domain.

growth interface can be seen. Then the top surface and cross-section of the sample were polished (Fig. 7(b) and (c)), and from SEM image, we can see clearly the phenomenon of ''push''. Regions free of Y211 inclusions (Fig. 7(e)) or regions with a little Y211 inclusions (Fig. 7(d)) are observed at the place of crystals, and beyond the front of growth interface, the region of a high density of Y211 particles is observed due to the effect of ''push'' force. The same phenomenon can be seen in the cross-section, and also can see clearly the liquid phase and the Y211 particles in front of the growth interface. Finally, we got the sample and proved that it's a single domain (Fig. 7(h)). The usual growth lines at the surface of the domains have been obtained. This has been confirmed using video imaging [14] of the melt growth process as the video recorded during this infiltration study.

4. Conclusions

Using the magnetic susceptibility measurements (MSM) method and in situ video observations, the phase transitions of bulk YBCO have been evidenced during the seeded infiltration growth (SIG) process. In the other word, melting and solidification are evidenced by the variation of the susceptibility at high temperature. With the lower heating rate, the temperature corresponding to the beginning of the melting and the initial nucleation point were shifted. The SIG mechanism

was investigated at different stages of the process. In addition, the single domain of the bulk YBCO was obtained. The results obtained in this first study of SIG by MSM and video observation can be improved in view of the large number of the parameters of the process: controlled atmosphere, slope of solidification ramp etc. and this opens interesting perspectives.

Acknowledgments

This work is supported by the CNRS/CRETA, CNRS/CRISMAT, and National Nature Science Foundation of China (50432050). Cao Haitao also acknowledges a fellowship from Chinese government.

References

[1] S. Meslin, J.G. Noudem, Infiltration and top seeded grown mono-domain YBaCuO bulk superconductor, Supercond. Sci. Technol. 17 (2004) 1324–1328.
[2] K. Iida, N. Hari Babu, Y. Shi, D.A. Cardwell, Seeded infiltration and growth of single-domain Gd–Ba–Cu–O bulk superconductors using a generic seed crystal, Supercond. Sci. Technol. 19 (2006) S478.
[3] S. Meslin, K. Iida, N. Hari Babu, D.A. Cardwell, J.G. Noudem, The effect of Y-211 precursor particle size on the microstructure and properties of Y–Ba–Cu–O bulk superconductors fabricated by seeded infiltration and growth, Supercond. Sci. Technol. 19 (2006) 711.
[4] Y.L. Chen, H.M. Chan, M.P. Harmer, V.R. Todt, S. Sengupta, D. Shi, A new method for net-shape forming of large, single-domain $YBa_2Cu_3O_{6+x}$, Physica C 234 (1994) 232–236.
[5] K Iida, N. Hari Babu, Y. Shi, D.A. Cardwell, Seeded infiltration and growth of large, single domain Y–Ba–Cu–O bulk superconductors with very high critical current densities, Supercond. Sci. Technol. 18 (2005) 1421.
[6] S. Jin, T.H. Tiefel, R.C. Sherwood, M.E. Davis, R.B. Van Dover, G.W. Kamlott, et al., High critical currents in yttrium barium copper oxide superconductors, Appl. Phys. Lett. 52 (1988) 2352.
[7] H. Fujimoto, M. Murakami, S. Gotoh, N. Koshizuka, T. Oyama, Y. Shiohara, S. Tanaka, Adv. Supercond. II (1990) 285.
[8] C. Leblond, et al., Effect of the oxygenation time and of the sample thickness on the levitation force of top seeding melt-processed YBCO, Supercond. Sci. Technol. 12 (1999) 405.
[9] M. Morita, S. Takebayashi, M. Tanaka, K. Kimura, K. Miyamoto, K. Sawano, Adv. Supercond. 3 (1991) 733.
[10] X. Chaud, D. Isfort, E. Beaugnon, R. Tournier, Isothermal growth of large $YBa_2Cu_3O_{7-x}$ single domains up to 93 mm, Physica C 2413 (2000) 341–348.
[11] E. Beaugnon, X. Chaud, P. De Rango, in: Yamaguchi Masuhiro, Tanimoto Yoshifumi (Eds.), Magneto-Science/Magnetic Field Effects on Materials Fundamentals and Applications, Kodansha Springer, Berlin, 2006, p. 179.
[12] X. Chaud, E. Beaugnon, R. Tournier, Magnetic susceptibility during the peritectic recombination of YBaCuO, Physica C 282-287 (1997) 525–526.
[13] X. Chaud, E. Beaugnon, P. De Rango, F. Ducloux, R. Tournier, P. Hiebel, P. Tixador, Y. Brunet, Role of oxygen on YBaCuO solidification as seen from high-temperature in-situ susceptibility measurements, Physica C 235 (1994) 433–434.
[14] Video at webpage: www-crismat.ensicaen.fr/crismat/crismat.html.